

The effect of Fe substitution on pyroelectric properties of $0.62\text{Pb}(\text{Mg}_{1/3}\text{Nb}_{2/3})\text{O}_3-0.38\text{PbTiO}_3$ single crystals

Xinming Wan^{a)}

The State Key Laboratory of High Performance Ceramics and Superfine Microstructure, Shanghai Institute of Ceramics, Chinese Academy of Sciences, 215 Chengbei Road Jiading, Shanghai 201800, China and Department of Applied Physics, The Hong Kong Polytechnic University, Hung Hom, Hong Kong, China

K.-H. Chew, H. L. W. Chan, and C. L. Choy

Department of Applied Physics, The Hong Kong Polytechnic University, Hung Hom, Hong Kong, China

Xiangyong Zhao and Haosu Luo

The State Key Laboratory of High Performance Ceramics and Superfine Microstructure, Shanghai Institute of Ceramics, Chinese Academy of Sciences, 215 Chengbei Road Jiading, Shanghai 201800, China

(Received 7 September 2004; accepted 29 December 2004; published online 9 March 2005)

Fe-doped $0.62\text{Pb}(\text{Mg}_{1/3}\text{Nb}_{2/3})\text{O}_3-0.38\text{PbTiO}_3$ (PMN-0.38PT) single crystals with two different dopant concentrations, 0.2 and 1.0 mol %, were grown by a modified Bridgman technique. The effect of Fe substitution on dielectric and pyroelectric properties was examined. The dielectric constant of the 0.2 mol % Fe-doped PMN-0.38PT single crystal was controlled successfully, indicating the possibility of tuning the dielectric properties by doping with a small concentration of iron ions. The mechanism of doping effect was also discussed based on the principles of crystal chemistry. The pyroelectric response of the single crystals was measured using a dynamic method from 20 to 50 °C. Compared with the 1.0 mol % Fe-doped single crystal, the 0.2 mol % Fe-doped sample possesses the better pyroelectric properties. At room temperature, the pyroelectric coefficient and detectivity figure of merit (F_D) for the 0.2 mol % Fe-doped sample are $568 \mu\text{C}/\text{m}^2 \text{K}$ and $53 \mu\text{Pa}^{-1/2}$, respectively, and they increase slightly with temperature increasing. These excellent pyroelectric properties as well as being able to produce large-size and high-quality single crystals make this kind of single crystal a promising candidate for high-performance infrared detectors and other pyroelectric applications. © 2005 American Institute of Physics.

[DOI: 10.1063/1.1862320]

I. INTRODUCTION

$(1-x)\text{Pb}(\text{Mg}_{1/3}\text{Nb}_{2/3})\text{O}_3-x\text{PbTiO}_3$ (PMN- x PT) single crystals are well-known ferroelectrics with perovskite structure and have come into prominence in the past few years due to their very high piezoelectric coefficients ($d_{33} > 2500 \text{ pC/N}$), extremely large piezoelectric strains ($> 1.7\%$), and extrahigh electromechanical coupling factor in the longitudinal bar mode ($k_{33} \sim 94\%$).¹⁻³ Such excellent properties point to a potential revolution in electromechanical transduction for a broad range of applications. Recently, many studies have focused on their optical properties.^{4,5} The result shows that PMN- x PT single crystals with tetragonal structure exhibit excellent electro-optic performance and are very promising candidates for optical devices.^{6,7}

The pyroelectric effect has been studied in many ferroelectric materials.⁸ While extensive studies on the properties of PMN- x PT single crystals have been made, less work has been performed on their pyroelectric response. It may be caused by their high dielectric constant which is unfavorable for pyroelectric applications. The properties of pyroelectric infrared detectors can be described by three major figures of merit (FOMs), as current response FOM F_i , voltage response FOM F_v , and detectivity FOM F_D .⁸ For high performance

pyroelectric detectors, high FOMs are required. Except for a high pyroelectric coefficient, an effective way to improve the FOMs is to reduce the dielectric constant and loss by controlling the microstructure of the materials.

It has been reported that for ferroelectric materials, small concentrations of substituents can dramatically influence their properties. Recently, Fe-doped $(1-x)\text{Pb}(\text{Zn}_{1/3}\text{Nb}_{2/3})\text{O}_3-x\text{PbTiO}_3$ (PZN- x PT) single crystals were grown and characterized.^{9,10} It was found that Fe substitution played a hardening effect and the dielectric constant for Fe-doped PZN- x PT single crystal in the tetragonal phase is much lower than that of undoped one. This may be related to the domain-wall pinning by the dipolar defects due to the presence of the dopants, which will suppress the dielectric constants. This leads to the idea in this work to reduce the dielectric constants by doping Fe ions in tetragonal PMN- x PT single crystals. The PMN-0.38PT single crystal has been studied widely as a typical composition with a tetragonal structure.^{5,7,11} The main objective of the present study is to investigate the possibility of tuning its dielectric and pyroelectric properties by doping iron ions. Fe-doped PMN-0.38PT single crystals with two different iron ion concentrations, 0.2 and 1.0 mol %, were grown and studied. Their figures of merit as pyroelectric detectors were also examined to explore their possible applications.

^{a)}Electronic mail: xmwan@citiz.net

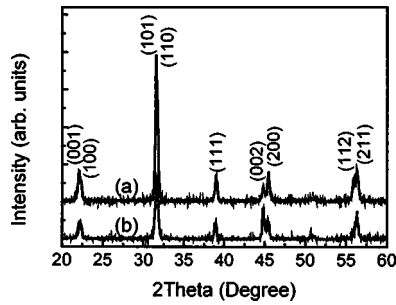


FIG. 1. Powder XRD patterns of Fe-doped PMN-0.38PT single crystals: (a) 0.2 mol % Fe-doped PMN-0.38PT and (b) 1.0 mol % Fe-doped PMN-0.38PT.

II. EXPERIMENTAL PROCEDURE

Fe-doped PMN-0.38PT single crystals were grown directly from melt by a modified Bridgman technique.^{2,12} The raw powders of Fe_2O_3 , PbO, MgO, Nb_2O_5 , and TiO_2 with purity of more than 99.99% were used as starting materials. B-site precursor synthesis method is used to prevent formation of the pyrochlore phase during crystal growth.¹³ A PMN-0.33PT single crystal was used as a seed crystal. Two kinds of crystals with different iron ion doping concentrations, 0.2 and 1.0 mol %, were prepared. Powder x-ray diffraction (XRD) analysis was performed by $\text{Cu } K\alpha$ radiation (Philips PW 3710 expert system).

It is known that for tetragonal PMN- x PT single crystals, the spontaneous polarization is along the $\langle 001 \rangle$ direction, so the samples were oriented and cut along this direction as confirmed by an x-ray diffractometer. Rectangular-shaped specimens of $6 \times 6 \times 0.6 \text{ mm}^3$ in dimension were prepared in this work. The samples were painted with silver paste and poled under an electric field of 1 kV/mm for 15 min at $\sim 160^\circ \text{C}$ in silicone oil. Using an Agilent 4294A precision impedance analyzer, the frequency dependence of dielectric behaviors was investigated in the range of 50–1000 Hz at room temperature. A dynamic method was used to measure the pyroelectric coefficient.^{14,15} In the measurement, the temperature of the sample was controlled by a Peltier heater and modulated sinusoidally with an amplitude of 1°C at a frequency of 5 mHz. The pyroelectric current was amplified by an electrometer and the 90° out-of-phase component modulated with respect to the temperature was measured with a digital lock-in amplifier.

III. RESULTS AND DISCUSSION

A. Powder XRD analysis and dielectric properties

Powder XRD analysis was performed to determine the phases in the as-grown Fe-doped PMN-0.38PT single crystals. The specimen was ground into fine powder. The XRD patterns obtained at room temperature are depicted in Fig. 1. The results show that both the single crystals possess the tetragonal structure and are free of the pyrochlore phase. It may be due to the seed crystal which had a key effect on restraining spontaneous nucleation and other parasitic growth.¹³

The dielectric properties of the Fe-doped PMN-0.38PT single crystals were examined with emphasis at the fre-

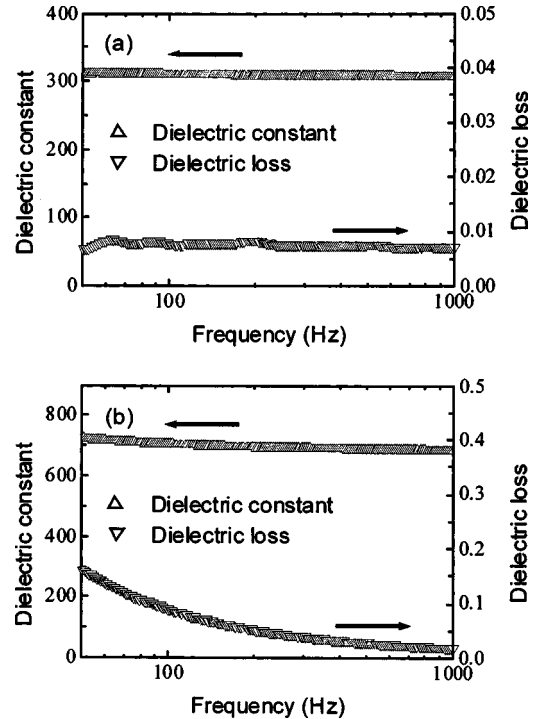


FIG. 2. Frequency dependence of the dielectric constant and loss of poled Fe-doped PMN-0.38PT single crystals at room temperature: (a) 0.2 mol % Fe-doped PMN-0.38PT and (b) 1.0 mol % Fe-doped PMN-0.38PT.

quency regime of 50–1000 Hz, as most of the applications of pyroelectric infrared detectors are in this frequency range. Figure 2 shows the frequency dependence of the dielectric constant and loss for poled Fe-doped PMN-0.38PT single crystals at room temperature. For the 0.2 mol % Fe-doped single crystal, as shown in Fig. 2(a), the dielectric constant and loss at 50 Hz are about 310 and 0.0067, respectively. They are almost invariable until 1 kHz. The dielectric constant reported at 1 kHz for a pure PMN-0.38PT single crystal is ~ 700 ,¹⁶ which is much higher than that of the 0.2 mol % Fe-doped sample. No value of the dielectric loss for a pure PMN-0.38PT single crystal has been reported. The result shows that the dielectric constant of a PMN-0.38PT single crystal is controlled successfully by doping with a small concentration of iron ions. For a higher doping concentration, the dielectric constant of the 1.0 mol % Fe-doped single crystal is about 725 at 50 Hz and decreases slightly with frequency increasing. The dielectric constants are similar with those of an undoped single crystal, but its dielectric losses are very high, which are more than 0.16 at 50 Hz. Though the dielectric loss decreases sharply with frequency increasing, it is still about 0.02 at 1 kHz, much higher than that of the 0.2 mol % Fe-doped one.

We now discuss the effect of iron ion substitution on the dielectric permittivity and loss of PMN-0.38PT single crystals. According to the principles of crystal chemistry, metallic ions prefer to enter sites with equal valence and similar radii. In the present study, the iron ions intend to substitute Ti^{4+} and produce oxygen vacancies, which form the $2\text{Fe}_{\text{Ti}}^{\times} - V_{\text{O}}^{\bullet}$ defect dipole pairs.¹⁰ The dipolar defects incline to align themselves in the direction of the polarization vector within domains, and this alignment will stabilize the domain struc-

ture. They may interact with polarization within a domain and make switching of the domain more difficult, effectively clamping the domain wall by the domain-wall pinning effects. The stabilization of domain structures leads to a decrease in dielectric permittivity and loss, as demonstrated in the Fe-doped PMN–0.38PT single crystal with a low doping concentration. However, for a higher iron ion doping concentration, the partial reduction of Fe^{3+} – Fe^{2+} might increase the hole conductivity of the single crystals, as in $\text{Pb}(\text{Fe}_{1/2}\text{Nb}_{1/2})\text{O}_3$ – $\text{Pb}(\text{Ni}_{1/3}\text{Nb}_{2/3})\text{O}_3$ (Ref. 17) and $\text{Pb}(\text{Fe}_{1/2}\text{Nb}_{1/2})\text{O}_3$ – $\text{Pb}(\text{Co}_{1/3}\text{Nb}_{2/3})\text{O}_3$ systems.¹⁸ This conductivity might contribute to the higher dielectric constant and loss, as reported in the $\text{Pb}(\text{Fe}_{1/2}\text{Nb}_{1/2})\text{O}_3$ – PbTiO_3 single crystal.¹⁹ The enhancement of dielectric permittivity and loss corresponding to the conductivity may be responsible for the results of the 1.0 mol % Fe-doped PMN–0.38PT single crystal, as shown in Fig. 2(b).

B. Pyroelectric properties

Let's see the effects of the iron ion substitution on the pyroelectric properties. A dynamic method was used to measure the pyroelectric coefficient in this work.^{14,15} In the traditional method, such as the Byer–Roundy method,²⁰ the pyroelectric coefficients consist of the contributions of nonpyroelectric currents, e.g., from thermally stimulated discharge. Using the dynamic technique, we can separate the real pyroelectric response from nonpyroelectric currents and obtain the pure pyroelectric coefficients.

At room temperature, the measured pyroelectric coefficient $-p$ for the 0.2 mol % Fe-doped PMN–0.38PT single crystal is $568 \mu\text{C}/\text{m}^2 \text{K}$, much higher than that of the 1.0 mol % Fe-doped one, $400 \mu\text{C}/\text{m}^2 \text{K}$. (The signs of the pyroelectric coefficients are defined according to the IRE standard.) The large value implies that the 0.2 mol % Fe-doped PMN–0.38PT single crystal is a very promising pyroelectric material. The unidirectional nonpyroelectric current due to space-charge relaxation or the leakage current which is the component of the current in phase with the temperature modulation has been separated from the true pyroelectric current. The coefficient due to the nonpyroelectric effect ($-p_{\text{non}}$) is 33 and $12 \mu\text{C}/\text{m}^2 \text{K}$ for the 0.2 and 1.0 mol % Fe-doped single crystals, respectively, which are both smaller than one-tenth of its $-p$. This indicates that the nonpyroelectric current only amounts to a very small part in the poled single crystals.

The temperature dependence of the pyroelectric properties was also characterized from 20 to 50 °C. After setting to a new temperature, the sample was kept for 15 min for the signal to become stable before the pyroelectric measurement was performed. The obtained pyroelectric coefficients of the

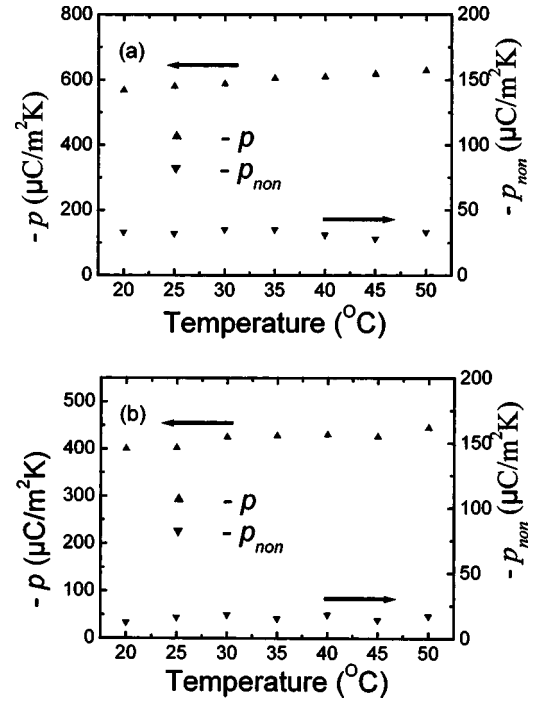


FIG. 3. Temperature dependence of the pyroelectric properties of Fe-doped PMN–0.38PT single crystals: (a) 0.2 mol % Fe-doped PMN–0.38PT and (b) 1.0 mol % Fe-doped PMN–0.38PT.

Fe-doped PMN–0.38PT single crystals as a function of temperature are shown in Fig. 3. The pyroelectric coefficient increases a little from 568 to $628 \mu\text{C}/\text{m}^2 \text{K}$ for the 0.2 mol % Fe-doped PMN–0.38PT single crystal, while the value of $-p_{\text{non}}$ remains almost constant. The 1.0 mol % Fe-doped single crystal has a similar variation with temperature. The temperature stability is also an important property of the single crystals for their applications in pyroelectric detectors.

FOMs are useful parameters for pyroelectric materials and are defined as follows: current response FOM $F_i = p/c_p$, voltage response FOM $F_v = p/(c_p \epsilon_0 \epsilon_r)$, and detectivity FOM $F_D = p/[c_p(\epsilon_0 \epsilon_r \tan \delta)^{1/2}]$. Here, c_p is the heat capacity per unit volume ($\sim 2.5 \times 10^6 \text{ J}/\text{m}^3 \text{ K}$).⁸ $\epsilon_0 = 8.85 \times 10^{-12} \text{ F}/\text{m}$ is the permittivity of free space. ϵ_r is the dielectric constant and $\tan \delta$ is the dielectric loss. The FOMs are often used to evaluate the pyroelectric properties and to judge the suitability of new materials for applications in pyroelectric infrared detectors. A summary of the dielectric properties, pyroelectric coefficients, and the calculated values of FOMs of the Fe-doped PMN–0.38PT single crystals at a frequency of 50 Hz is given in Table I. The values of $-p$ and FOMs for the 0.2 mol % Fe-doped single crystal are all much higher than those of the 1.0 mol % Fe-doped one, indicating the better pyroelectric properties for the PMN–0.38PT single crystal

TABLE I. The values of the pyroelectric coefficient, dielectric properties, and various FOMs at room temperature for Fe-doped PMN–0.38PT single crystals.

Concentration	ϵ_r (50 Hz)	$\tan \delta$ (50 Hz)	$-p$ ($\mu\text{C}/\text{m}^2 \text{K}$)	F_i (pm/V)	F_v (m^2/C)	F_D ($\mu\text{Pa}^{-1/2}$)
0.2 mol % Fe	310	0.0067	568	227.2	0.083	53
1.0 mol % Fe	725	0.161	400	160	0.025	5

with a low doping concentration. Besides, it also shows the possibility of tailoring the pyroelectric coefficient and FOMs by doping iron ions. Compared with the reported values of $-p$ and F_D for the widely used pyroelectric single-crystal LiTaO_3 ($230 \mu\text{C}/\text{m}^2 \text{K}$ and $49 \mu\text{Pa}^{-1/2}$),^{8,21} the 0.2 mol % Fe-doped PMN–0.38PT single crystal also has higher values of $568 \mu\text{C}/\text{m}^2 \text{K}$ and $53 \mu\text{Pa}^{-1/2}$, respectively. These excellent pyroelectric properties, as well as being able to obtain large-size and high-quality single crystals, make the 0.2 mol % Fe-doped PMN–0.38PT single crystal a very promising candidate for uncooled infrared detectors and thermal imaging applications.

IV. CONCLUSION

Two kinds of Fe-doped PMN–0.38PT single crystals with different iron ion molar ratios, 0.2 and 1.0 mol %, were grown by means of a modified Bridgman technique. The effect of Fe substitution on dielectric and pyroelectric properties was examined by single crystals poled along the spontaneous polarization direction. The dielectric permittivity of the 0.2 mol % Fe-doped PMN–0.38PT single crystals is much lower than that of the undoped single crystal, which indicates the successful adjustment of dielectric properties by doping with a small concentration of iron ions. This may be related to the domain-wall pinning by the dipolar defects due to the presence of the dopants, which will suppress the dielectric constants. However, for a higher iron ion doping concentration, the dielectric constant and loss both increase because the partial reduction of Fe^{3+} – Fe^{2+} might increase the conductivity of the single crystals.

The pyroelectric response of the single crystals was measured using a dynamic method from 20 to 50 °C. Compared with the 1.0 mol % Fe-doped single crystal, the 0.2 mol % Fe-doped sample possesses the higher pyroelectric coefficient and FOMs. At room temperature, the measured pyroelectric coefficient and detectivity figure of merit F_D for the 0.2 mol % Fe-doped PMN–0.38PT single crystal are $568 \mu\text{C}/\text{m}^2 \text{K}$ and $53 \mu\text{Pa}^{-1/2}$, respectively, both better than those of the widely used pyroelectric single crystal LiTaO_3 . Since large-size and high-quality single crystals can be ob-

tained, these excellent pyroelectric properties, including their temperature stability, make the 0.2 mol % Fe-doped PMN–0.38PT single crystal a promising candidate for high-performance infrared detectors and other pyroelectric applications.

ACKNOWLEDGMENTS

This work is supported by the National Natural Science Foundation of China (Grant No. 50272075), the High Technology and Development Project of the People's Republic of China (Grant No. 2002AA325130), the Hong Kong Research Grants Council (PolyU Grant No. 5193/00P), and the Centre for Smart Materials of the Hong Kong Polytechnic University.

¹R. F. Service, *Science* **275**, 1878 (1997).

²Z. Yin, H. Luo, P. Wang, and G. Xu, *Ferroelectrics* **299**, 207 (1999).

³S.-E. Park and T. R. Shrout, *J. Appl. Phys.* **82**, 1804 (1997).

⁴X. Wan, H. L. W. Chan, C. L. Choy, X. Zhao, and H. Luo, *J. Appl. Phys.* **96**, 1387 (2004).

⁵X. Wan, H. Luo, J. Wang, H. L. W. Chan, and C. L. Choy, *Solid State Commun.* **129**, 401 (2004).

⁶D.-Y. Jeong, Y. Lu, V. Sharma, Q. Zhang, and H. Luo, *Jpn. J. Appl. Phys., Part 1* **42**, 4387 (2003).

⁷X. Wan, H. Xu, T. He, D. Lin, and H. Luo, *J. Appl. Phys.* **93**, 4766 (2003).

⁸R. W. Whatmore, *Rep. Prog. Phys.* **49**, 1335 (1986).

⁹S. Priya, K. Uchino, and D. Viehland, *Appl. Phys. Lett.* **81**, 2430 (2002).

¹⁰S. Zhang, L. Laurent, D. Y. Jeong, C. A. Randall, Q. Zhang, and T. R. Shrout, *J. Appl. Phys.* **93**, 9257 (2003).

¹¹X. Wan, T. He, D. Lin, H. Xu, and H. Luo, *Acta Phys. Sin.* **52**, 2319 (2003).

¹²X. Wan, J. Wang, H. L. W. Chan, C. L. Choy, H. Luo, and Z. Yin, *J. Cryst. Growth* **263**, 251 (2004).

¹³M. Orita, H. Satoh, and K. Aizawa, *Jpn. J. Appl. Phys., Part 1* **31**, 3261 (1992).

¹⁴L. E. Garn and E. J. Sharp, *J. Appl. Phys.* **53**, 8974 (1982).

¹⁵E. J. Sharp and L. E. Garn, *J. Appl. Phys.* **53**, 8980 (1982).

¹⁶H. Cao and H. Luo, *Ferroelectrics* **274**, 309 (2002).

¹⁷T. R. Shrout, S. L. Swartz, and M. J. Haun, *Am. Ceram. Soc. Bull.* **63**, 808 (1984).

¹⁸K. B. Park and K. H. Yoon, *Ferroelectrics* **145**, 195 (1993).

¹⁹Y. Gao, H. Xu, Y. Wu, T. He, G. Xu, and H. Luo, *Jpn. J. Appl. Phys., Part 1* **40**, 4998 (2001).

²⁰R. L. Byer and C. B. Roundy, *Ferroelectrics* **3**, 333 (1972).

²¹R. W. Whatmore, P. C. Osbond, and N. M. Shorrocks, *Ferroelectrics* **76**, 351 (1987).

Journal of Applied Physics is copyrighted by the American Institute of Physics (AIP). Redistribution of journal material is subject to the AIP online journal license and/or AIP copyright. For more information, see <http://ojps.aip.org/japo/japcr/jsp>